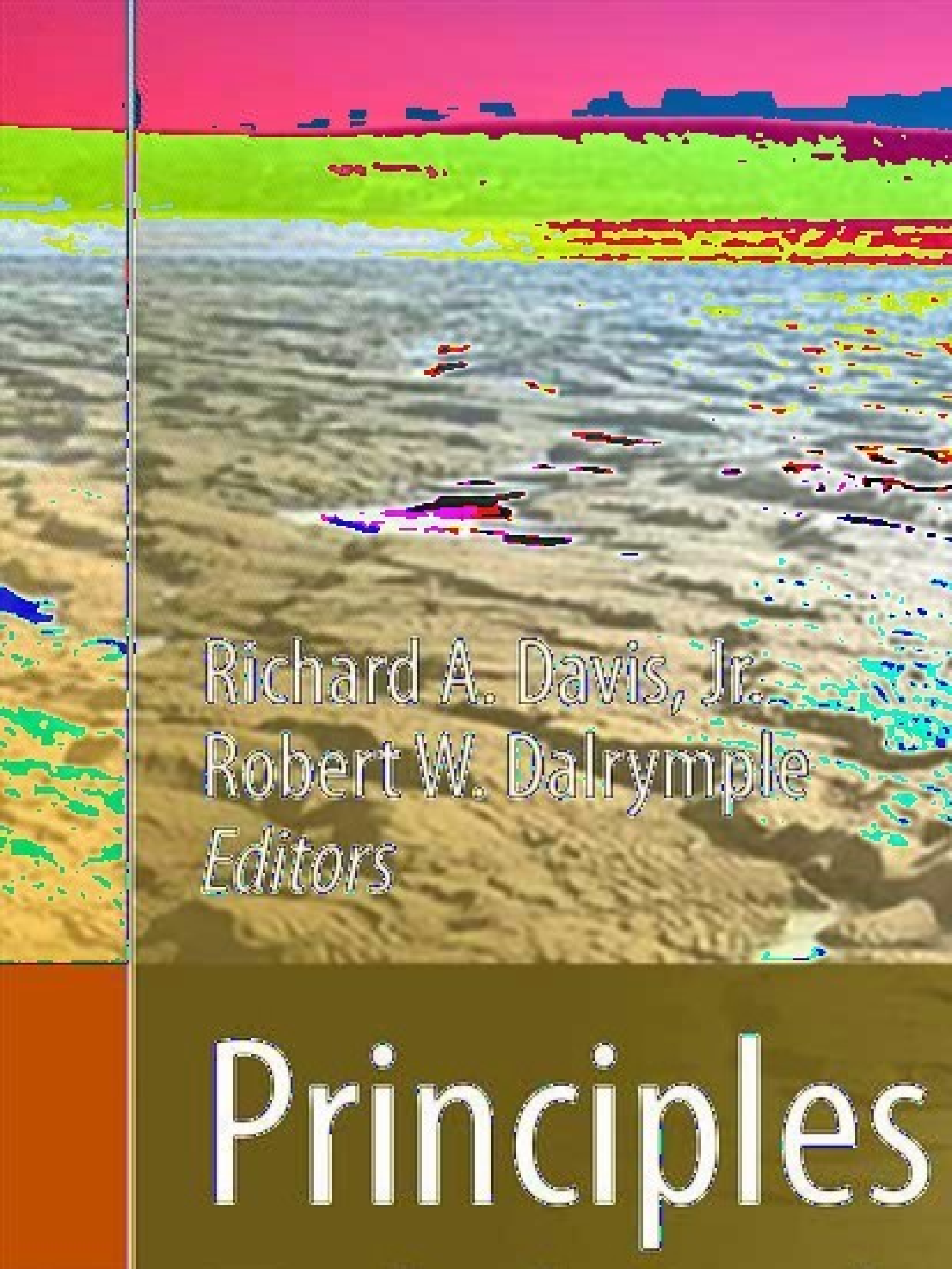
Richard A. Davis, Jr.
Robert W. Dalrymple
Editors
Principles

Principles of Tidal Sedimentology

Richard A. Davis, Jr. • Robert W. Dalrymple
Editors

Principles of Tidal Sedimentology

Springer

Editors
Richard A. Davis, Jr.
Harte Research Institute
Texas A&M University
Ocean Drive 6300
Corpus Christi, TX 78412
USA

Coastal Research Laboratory
Department of Geology
University of South Florida
Tampa, FL 33620
rdavis@usf.edu

Robert W. Dalrymple
Department of Geological Sciences and
Geological Engineering
Queen's University
Miller Hall
Kingston, ON K7L 3N6
Canada
dalrymple@geol.queensu.ca

ISBN 978-94-007-0122-9 e-ISBN 978-94-007-0123-6
DOI 10.1007/978-94-007-0123-6
Springer Dordrecht Heidelberg London New York

Library of Congress Control Number: 2011939475

© Springer Science+Business Media B.V. 2012
No part of this work may be reproduced, stored in a retrieval system, or transmitted in any form or by any means, electronic, mechanical, photocopying, microfilming, recording or otherwise, without written permission from the Publisher, with the exception of any material supplied specifically for the purpose of being entered and executed on a computer system, for exclusive use by the purchaser of the work.

Cover illustration: Fig. 5.13 (upper part) from this book.

Printed on acid-free paper

Springer is part of Springer Science+Business Media (www.springer.com)

Preface

Tides have fascinated humans for millennia. Their regularity and their apparent correlation with lunar behavior intrigued natural philosophers, even the Greeks, who live on an essentially tideless sea although there are strong tidal currents in localized constrictions. Apparently, they learned about tides from areas outside the Straits of Gibralter and from the Arabs who experienced significant tides in the Persian Gulf. From a practical perspective, tidal changes in water elevation and the currents associated with these changes were of great importance for shipping and military purposes. In areas such as the countries surrounding the southern North Sea, such considerations required accurate tidal predictions, which in turn drew the attention of some of the greatest astronomers and mathematicians.

Among the notable individuals who devoted at least part of their careers to the study of tides, and have contributed to our understanding of them are Galileo, Descartes, Bacon, Kepler, Euler, Laplace, and Lord Kelvin (Cartwight 1999). Indeed, many of the widely used mathematical techniques that we now take for granted were developed to help understand the behavior of the tides. More recently, interest in tides and storm surges has been fostered by the need to protect ever-increasing coastal population centers from catastrophic inundation, and by the desire to "reclaim" tidal flats for agricultural and industrial purposes. Foremost in this activity have been The Netherlands, Germany, and adjacent parts of Denmark.

Research on the nature of tidal deposits has been underway for about 50 years. Early studies on the Wadden Sea along the North Sea coast of The Netherlands and Germany were among the original landmark efforts in this area (e.g. van Straaten 1954; Postma 1961; Reineck 1963), and were followed closely by work in England (Evans 1965) and France (Bajard 1966). Such efforts were driven by the dual need to understand the coastal zone for the protection of population centers and to provide an actualistic analog for ancient sedimentary successions. In North America, Klein's work on the Bay of Fundy (Klein 1963) initiated detailed efforts in that part of the world. The early German work in the North Sea had a major biological and ichnological component, a topic that was pursued systematically at the Skidaway Institute of Oceanography in the southeastern United States (e.g. Frey and Howard 1969). Despite having some of the most widespread tidal flats in the world, work along the Chinese coast was relatively slow to develop, although there were notable early studies (e.g. Wang 1963). In the carbonate realm, pioneering studies were conducted on the tidal flats of Andros Island, the Bahamas (e.g. Shinn et al. 1969), and the Persian Gulf (Evans et al. 1969).

In spite of important work on the shallow-marine tidal deposits in the seas of northwestern Europe (e.g. Stride 1963), most of the early work on modern tidal

deposits was devoted to study of intertidal environments, mainly because they were readily accessible. This fixation on the intertidal zone is perhaps nowhere more evident in the influential compilation of examples contained in the book *Tidal Deposits: A Casebook of Recent Examples and Fossil Counterparts* (Ginsburg 1975). Indeed, the upward-fining succession developed by the progradation of a tidal flat was among the very first facies models created. Application of these studies to the rock record was widespread in the carbonate literature, with numerous documented examples being published through the 1960s, 1970s and 1980s. By comparison, the extension of the work on the modern tidal deposits to ancient siliciclastic successions was slow. At least one impediment to the widespread application to the ancient was the notion put forward by Irwin (1965), and since largely disproven, at least for siliciclastic sediments, that the expansive epicontinental seas of the past were largely tideless, as a result of frictional damping of the tidal wave. An even greater impediment was the lack of definitive criteria for the recognition of tidal deposits, given that exposure indicators are much less easily preserved in siliciclastic tidal deposits than they are in carbonates. Thus, a milestone in the study of tidal deposits occurred in 1980 with the publication by Visser (1980) of "tidal bundles" in cross beds formed by subaqueous dunes, which provided the first documentation of a definitive indicator of tidal sedimentation, spawned the widespread recognition of ancient tidal deposits in an ever-growing number of localities.

Gradually, the focus of research on modern tidal environments has shifted away from tidal flats, toward a more comprehensive examination of tidal sedimentation in a wide range of settings, including even the deep ocean. Studies have tended to become more holistic in their treatment of entire depositional systems, rather than concentrating on only one part (e.g. tidal flats) of the whole. This more comprehensive approach is evident in many of the papers in this volume.

Because of the increasing attention given to tidal deposits it became important to organize a uniform nomenclature and approach to their study. As a consequence, Robert N. Ginsburg organized and hosted a conference of interested researchers in February of 1973. It included field experiences in both siliciclastic (Sapelo Island, Georgia, USA) and carbonate areas (Florida Keys, USA and the Bahamas), followed by presentations of research on "tidalites" (a term coined by George deVries Klein (1971)) by all in attendance. The next similar conference was held in The Netherlands in 1986, followed in regular succession by a series International Conferences on Tidal Sedimentology that has met in Calgary, Canada (1989), Wilhelmshaven, Germany (1992), Savannah, Georgia USA (1996), Seoul, Korea (2000), Copenhagen, Denmark (2004) and, most recently, in Qingdao, China (2008). The next meeting will be in Caen, France in 2012.

The meeting in 2008 in China was particularly stimulating with an attendance that surpassed any previous meeting. The expansion of interest in tidal deposits appears to be spurred by two factors: the need to understand coastal tidal environments in order to predict how these sensitive environments might respond to sea-level rise and climate change; and providing data and interpretations to help in understanding ancient depositional environments that were influenced by tides. Davis thought it was a good time to assemble a principles-type volume on the topic of tidal sedimentology given that no such synthesis exists, and because there has been so much new research on tidal environments and deposits over the last few years. Dalrymple agreed to be co-editor and the result of their efforts is this volume.

The purpose of this volume is to provide the first-ever, high-level overview of tidal sedimentology. Many of the chapters contain the first-ever synthesis of information

on the particular topic! The approach is comprehensive with state-of-the-art reviews of the full spectrum of tidal depositional environments, from supratidal salt marshes, through the full range of coastal environments and continental shelves, to the deep sea. Examples from modern environments and ancient deposits are provided, and both siliciclastic and carbonate environments are discussed. The book is organized in the following four parts. (1) Chapters 1–4 provide overviews of the fundamentals of: the generation of tides, the nature of sediment transport by tidal currents, the criteria by which tidal deposits can be recognized, and the ichnology of tidal deposits. The later chapter represents the first time that the ichnological characteristics of tidal deposits have been reviewed systematically. (2) Chapters 5–14 review the characteristics of the full range of siliciclastic tidal environments, including both tide-dominated estuaries and deltas, as well as the various tidal components of barrier-lagoon systems. These chapters cover all aspects of the sedimentology of these environments, from the details of the physical processes operating in them, through the morphodynamics and facies, and the stratigraphic organization of the deposits. (3) Chapters 15–18 provide syntheses of particular times and places in earth history where tidal deposits are particularly notable. The chapter on the Precambrian reviews tidal sedimentation at a time when the Moon was significantly closer to the Earth and the tide-generating force should have been stronger. The reviews of the tidal deposits in the Illinois Basin (Carboniferous age), Western Interior Seaway (Cretaceous) and Spanish Pyrenean Basin (Eocene) provide unique insights into the large-scale (tectonic and relative sea level) controls on the spatial and temporal distribution of tidal sedimentation. (4) Chapters 19–21 discuss tidal sedimentation in modern and ancient carbonate environments.

Experts from throughout the world have been chosen to be the lead authors on each of the chapters. They and their co-authors build on their considerable personal experience to present insightful syntheses of the latest research in the particular topic. Each chapter has abundant illustrations, many of which are in color to enhance their effectiveness. References are extensive and include historically important ones as well as those on the leading edge of each topic.

Because of the uniquely broad coverage within each of the chapters, and in the volume as a whole, this book should be of value to a wide range of researchers. Workers who study modern sedimentary environments, and especially coastal settings, including environmental managers and coastal engineers, will find much about the dynamics of these environments that will assist them to develop protection strategies that are compatible with the natural behavior of these complex systems, including their response to potentially rising sea level. Geologists who study ancient sedimentary successions, whether for more academic or more applied reasons, will find a wealth of information about the behavior of tidal environments, ranging from the nature of the facies, through small-scale sedimentary successions, to the largest-scale sequence-stratigraphic control on tidal sedimentation.

The editors and authors gratefully acknowledge the financial support of numerous funding agencies that have provided support for their respective research activities. They also thank the people who have provided excellent and constructive reviews (see below). The editors appreciate the cooperation of Dr. Robert Doe and his staff at Springer Publishers.

Chapter Reviewers

Clark Alexander
Serge Berné
Sean Bingham
Ron Boyd
Margie Chan
Kyungsik Choi
Poppe de Boer
Robert Dott
Paul Enos
Jon French
Shu Gao
Murray Gingras
Liviu Giosan
Steven Greb
Gary Hampson
Steve Hasiotis
Christopher Kendall
George Klein
Erik Kvale
Tim Lawton
Don McNeil
Bruce Nocita
Nora Noffke
David Piper
Piret Plink-Bjorklund
Brian Pratt
Denise Reed
Joshiki Saito
Gene Shanmugam
Gene Shinn
Ronald Steel
John Suter
S. Temmerman
Bernadette Tessier
Ad van der Spek
Grant Wach
Ping Wang
Colin Woodruff
Paul Wright

References

Bajard J (1966) Figure et structures sédimentaires dans la partie orientale de la baie de Mont Saint-Michel. Rev Geog Phys Geol Dyn 8:39–112

Cartwright DE (1999) Tides: a scientific history. Cambridge University Press, Cambridge, 292 p

Evans G (1965) Intertidal flat sediments and their environments of deposition in The Wash. J Geol Soc Lond 121:209–245

Evans G, Schmidt V, Bush P, Nelson H (1969) Stratigraphy and geologic history of the Sabkha, Persian Gulf. Sedimentology 12:145–159

Frey RW, Howard JD (1969) A profile of biogenic sedimentary structures in a Holocene barrier island-salt marsh complex, Georgia. Gulf Coast Assoc Geol Soc Trans 19:427–444

Ginsburg RN (1956) Environmental relationships of grain size and constituent particles in some south Florida carbonate sediments. Bull Am Assoc Petrol Geol 40:2384–2427

Ginsburg RN (1975) Tidal deposits: a casebook of recent examples and fossil counterparts. Springer, New York, 426 p

Irwin ML (1965) General theory of epeiric clear water sedimentation. Bull Am Assoc Petrol Geol 49: 445–459

Klein deV G (1971) A sedimentary model for determining paleotidal range. Geol Soc Am Bull 82:2585–2592

Postma H (1961) Transport and accumulation of suspended matter in the Dutch Wadden Sea. Neth J Sea Res 1:148–190

Reineck H-R (1963) Sedimentgefüge im Bereich der südlichen Nordsee. Abhandl Senckenber Naturforsch Ges 505:1–138

Shinn EA, Lloyd RM, Ginsburg RN (1969) Anatomy of a modern carbonate tidal flat, Andros Island, Bahamas. J Sediment Petrol 39:112–123

Stride AH (1963) Current-swept sea floors near the southern half of Great Britain. Q J Geol Soc Lond 119:175–199

van Straaten LMJU (1954) Composition and structure of recent marine sediments in the Netherlands. Leidse Geol Mededel 19:1–110

Visser MJ (1980) Neap-spring cycles reflected in Holocene subtidal large-scale bedform deposits: a preliminary note. Geology 8:543–546

Wang Y (1963) The coastal dynamic geomorphology of the northern Bohai Bay. In: Wang Y (ed) Collected oceanic works of Nanjing University. Nanjing University Press, Nanjing (in Chinese with English abstract)

Corpus Christi, Texas USA
Kingston, Ontario, Canada

Contents

1 Tidal Constituents of Modern and Ancient Tidal Rhythmites: Criteria for Recognition and Analyses 1
Erik P. Kvale

2 Principles of Sediment Transport Applicable in Tidal Environments 19
Ping Wang

3 Tidal Signatures and Their Preservation Potential in Stratigraphic Sequences 35
Richard A. Davis, Jr.

4 Tidal Ichnology of Shallow-Water Clastic Settings 57
Murray K. Gingras and James A. MacEachern

5 Processes, Morphodynamics, and Facies of Tide-Dominated Estuaries 79
Robert W. Dalrymple, Duncan A. Mackay, Aitor A. Ichaso, and Kyungsik S. Choi

6 Stratigraphy of Tide-Dominated Estuaries 109
Bernadette Tessier

7 Tide-Dominated Deltas 129
Steven L. Goodbred, Jr. and Yoshiki Saito

8 Salt Marsh Sedimentation 151
Jesper Bartholdy

9 Open-Coast Tidal Flats 187
Daidu Fan

10 Siliciclastic Back-Barrier Tidal Flats 231
Burghard W. Flemming

11 Tidal Channels on Tidal Flats and Marshes 269
Zoe J. Hughes

12 Morphodynamics and Facies Architecture of Tidal Inlets and Tidal Deltas 301
Duncan FitzGerald, Ilya Buynevich, and Christopher Hein

13 Shallow-Marine Tidal Deposits 335
Jean-Yves Reynaud and Robert W. Dalrymple

14 Deep-Water Tidal Sedimentology 371
Mason Dykstra

15 Precambrian Tidal Facies. 397
Kenneth A. Eriksson and Edward Simpson

16 Hypertidal Facies from the Pennsylvanian Period: Eastern and Western Interior Coal Basins, USA 421
Allen W. Archer and Stephen F. Greb

17 Tidal Deposits of the Campanian Western Interior Seaway, Wyoming, Utah and Colorado, USA 437
Ronald J. Steel, Piret Plink-Bjorklund, and Jennifer Aschoff

18 Contrasting Styles of Siliciclastic Tidal Deposits in a Developing Thrust-Sheet-Top Basins – The Lower Eocene of the Central Pyrenees (Spain) 473
A.W. Martinius

19 Holocene Carbonate Tidal Flats 507
Eugene C. Rankey and Andrew Berkeley

20 Tidal Sands of the Bahamian Archipelago 537
Eugene C. Rankey and Stacy Lynn Reeder

21 Ancient Carbonate Tidalites 567
Yaghoob Lasemi, Davood Jahani, Hadi Amin-Rasouli, and Zakaria Lasemi

Index. 609

Contributors

Hadi Amin-Rasouli Department of Geosciences, University of Kurdistan, Sanandaj, Iran, H.Aminrasouli@uok.ac.ir

Allen W. Archer Department of Geology, Kansas State University, Manhattan, KS 66506, USA, aarcher@ksu.edu

Jennifer Aschoff Department of Geology and Geologic Engineering, Colorado School of Mines, Golden, CO, USA, jaschoff@mines.edu

Jesper Bartholdy Department of Geography and Geology, University of Copenhagen, 10 Øster Voldgade, Copenhagen DK-3050, Denmark, jb@geogr.ku.dk

Andrew Berkeley Department of Evironmental & Geographical Sciences, Manchester Metropolitan University, John Dalton Extension Building, Chester Street, Manchester M1 5GD, UK

Ilya Buynevich Department of Earth and Environmental Sciences, Temple University, 313 Philadelphia, PA 19122, USA, coast@temple.edu

Kyungsik S. Choi Faculty of Earth Systems and Environmental Sciences, Chonnam National University, Gwangju 500-757, South Korea, tidalchoi@hotmail.com

Robert W. Dalrymple Department of Geological Sciences and Geological Engineering, Queens University, Kingston, ON K7L 3N6, Canada, dalrymple@geol.queensu.ca

Richard A. Davis, Jr. Department of Geology, Coastal Research Laboratory, University of South Florida, Tampa, FL 33620, USA, rdavis@usf.edu

Harte Research Institute for Gulf of Mexico Studies, Texas A&M University – Corpus Christi, TX 78412, USA

Mason Dykstra Department of Geology and Geological Engineering, Colorado School of Mines, Golden, CO 80401, USA, mdykstra@mines.edu

Kenneth A. Eriksson Department of Geosciences, Virginia Tech, Blacksburg, VA 24061, USA, kaeson@vt.edu

Daidu Fan State Key Laboratory of Marine Geology, Tongji University, Shanghai 200092, China, ddfan@tongji.edu.cn

Duncan FitzGerald Department of Earth Sciences, Boston University, Boston, MA 02215, USA, dunc@bu.edu

Burghard W. Flemming Senckenberg Institute, Suedstrand 40, 26382 Wilhelmshaven, Germany, bflemming@senckenberg.de

Murray K. Gingras Department of Earth and Atmospheric Sciences, University of Alberta, Edmonton, AB T6G 2E3, Canada, mgingras@ualberta.ca

Steven L. Goodbred, Jr. Department of Earth and Environmental Sciences, Vanderbilt University, Nashville, TN 37240, USA, steven.goodbred@vanderbilt.edu

Stephen F. Greb Kentucky Geological Survey, University of Kentucky, Lexington, KY 40506, USA, greb@uky.edu

Christopher Hein Department of Earth Sciences, Boston University, Boston, MA 02215, USA, hein@whoi.edu

Zoe J. Hughes Department of Earth Sciences, Boston University, Boston, MA 01778, USA, zoeh@bu.edu

Aitor A. Ichaso Department of Geological Sciences and Geological Engineering, Queens University, Kingston, ON K7L 3N6, Canada, aitorichaso@hotmail.com

Davood Jahani Department of Geology, Faculty of Basic Sciences, North Tehran Branch, Islamic Azad University, Tehran, Iran, d_jahani@iau-tnb.ac.ir

Erik P. Kvale Devon Energy Corporation, 20 North Broadway, Oklahoma City, OK 73102, USA, Erik.Kvale@dvn.com

Yaghoob Lasemi Illinois State Geological Survey, Prairie Research Institute, University of Illinois at Urbana-Champaign, Champaign, IL 61820, USA, ylasemi@illinois.edu

Zakaria Lasemi Illinois State Geological Survey, Prairie Reserarch Institute, University of Illinois at Urbana-Champaign, Champaign, IL 61820, USA, zlasemi@illinois.edu

James A. MacEachern Department of Earth Sciences, Simor Fraser Univeraity, 8888 University Drive, Burnaby, BC V5A 1S6, Canada, jmaceach@suf.ca

Duncan A. MacKay Department of Geological Sciences and Geological Engineering, Queens University, Kingston, ON K7L 3N6, Canada, duncanamackay@yahoo.com

A.W. Martinius Statoil Research and Development, Arkitekt Ebbels vei 10, N-7005 Trondheim, Norway, awma@Statoil.com

Piret Plink-Bjorklund Department of Geology and Geologic Engineering, Colorado School of Mines, Golden, CO, USA, pplink@mines.edu

Eugene C. Rankey Department of Geology, University of Kansas, 1475 Jayhawk Blvd., 120 Lindley Hall, Lawrence, KS 66045, USA, grankey@ku.edu

Stacy Lynn Reeder Schlumberger-Doll Research, One Hampshire Street, Cambridge, MA 02139, USA, sreeder@slb.com

Jean-Yves Reynaud Département Histoire de la Terre – UMR 7193 ISTeP, Muséum National d'Histoire Naturelle, Géologie, CP 48, 43, rue Buffon, F-75005 Paris, France, jyr@mnhn.fr

Yoshiki Saito Geological Survey of Japan, AIST, Central 7, Higashi 1-1-1, Tsukuba 305-8567, Japan, yoshiki.saito@aist.go.jp

Edward Simpson Department of Physical Sciences, Kutztown University, Kutztown, PA 19530, USA, simpson@kutztown.edu

Ronald J. Steel Department of Geological Sciences, University of Texas – Austin, Austin, TX 78712, USA, rsteel@mail.utexas.edu

Bernadette Tessier Morphodynamique Continentale et Côtière, University of Caen, UMR CNRS 6143, 24 Rue des Tilleuls, 14000 Caen, France, bernadette.tessier@unicaen.fr

Ping Wang Coastal Research Laboratory, Department of Geology, University of South Florida, Tampa, FL 33620, USA, pwang@usf.edu

Tidal Constituents of Modern and Ancient Tidal Rhythmites: Criteria for Recognition and Analyses

1

Erik P. Kvale

Abstract

The origin of oceanic tides is a basic concept taught in most introductory college-level sedimentology, geology, oceanography, and astronomy courses. Tides are commonly explained in the context of the equilibrium-tidal theory model. The equilibrium model explains tides in the context of changes in two hemisphere-opposite tidal bulges through which the Earth spins. The position and size of these tidal bulges relative to the Earth's equator is largely controlled by the phases of the Moon and changes in declination and orbital distance of the Moon in its orbit around the Earth. While explaining the driving forces that cause tides, the equilibrium model does not explain most of the tides observed in the Earth's oceans.

A complete explanation of the origin of tides must include a discussion of dynamic tidal theory. In the dynamic tidal model, tides resulting from the motions of the Moon in its orbit around the Earth and the Earth in its orbit around the Sun are modeled as products of the combined effects of a series of phantom satellites. The movement of each of these satellites, relative to the Earth's equator, creates its own tidal wave that moves around an amphidromic point. Each of these waves is referred to as a tidal "constituent" or "species." The geometries of the ocean basins determine which of these constituents are amplified. Thus, the tide-raising potential for any locality on Earth can be conceptualized as the summation of the amplitudes of a series of tidal constituents specific to that region. A better understanding of tidal cycles opens up remarkable opportunities for research on tidal deposits with implications for, among other things, a more complete understanding of the tidal dynamics responsible for sediment transport and deposition, tectonic-induced changes in paleogeographies, and changes in Earth–Moon distance through time.

1.1 Introduction

Tidal rhythmites, small-scale sedimentary structures that include thinly layered, fine grained sediments, record, through the cyclic variations in the thicknesses of successive laminae, changes in current velocities associated with lunar/solar cycles. The thickness of a

E.P. Kvale (✉)
Devon Energy Corporation, 20 North Broadway, Oklahoma City, OK 73102, USA
e-mail: Erik.Kvale@dvn.com

R.A. Davis, Jr. and R.W. Dalrymple (eds.), *Principles of Tidal Sedimentology*,
DOI 10.1007/978-94-007-0123-6_1, © Springer Science+Business Media B.V. 2012

lamina is directly and positively related to tidal current strength, which in turn is directly and positively related to the magnitude of the daily rise and fall of the tide (tidal range). Over periods of days, months, or years, changes in tidal current strengths associated with various lunar/solar cycles are mirrored by the change in thicknesses of the vertically stacked laminae.

Modern and ancient tidal rhythmites have been found on every continent in the world except Antarctica. In modern environments, tidal rhythmites occur in deposits associated with tide-dominated deltas, tidal embayments, and estuaries. Tidal rhythmites can be used for reconstructing ancient paleogeographies and paleoclimates (e.g. this chapter, Hovikoski et al. 2005; Kvale et al. 1994), estimating paleotidal ranges (e.g. Archer 1995; Archer and Johnson 1997), understanding channel migration in the fluvio-estuaring transition (Choi 2010) determining lunar-retreat rates through time (e.g. Williams 1989; Kvale et al. 1999), and most recently, have been used to infer the major tidal constituents associated with the tides that deposited them (e.g. Kvale 2006). In order to understand tidal rhythmites, however, one has to understand how tides are generated and what controls their genesis.

The impact of diurnal, semidiurnal, and semimonthly (neap-spring) tidal cycles on sediment deposition has been well documented since the early 1980s (e.g. Visser 1980; Boersma and Terwindt 1981; Allen 1981). For many geologists these became benchmark papers when they were published because they showed how depositional packages within sedimentary successions can be linked to a tidal origin. However, it was the discovery of modern and ancient tidal rhythmites in the late 1980s and 1990s that showed that a hierarchy of tidal cycles, beyond simple semidaily, daily or fortnightly events, could be preserved in the rock record (e.g. Kvale et al. 1989; Williams 1989; Dalrymple and Makino 1989; Archer et al. 1991; Kvale et al. 1994; Miller and Eriksson 1997). Tidal cycles associated with monthly, semiannual, annual (usually includes a significant seasonal climatic component), and even an approximately 18-year cycle have been identified from ancient tidal rhythmites.

Studies, however, showed that the understanding of one of the most basic of the tidal cycles, the neap-spring or fortnightly tidal cycle, by most geologists, and apparently many oceanographers, and astronomers as well, was over-simplified. Many college-level textbooks today continue to propagate a basic misunderstanding of the neap-spring cycles and the origin of oceanic tides in general (e.g. Duxbury et al. 2002).

The intent of this chapter is neither to outline a history of the study of tides and tidal deposits nor to document the current state of knowledge regarding the history of the Earth-Moon system. These issues are treated in some detail in Klein (1998), Rosenberg (1997), Williams (2000), and Coughenour et al. (2009). Rather, it is to explain some basic tidal theory and show how a more complete knowledge of ancient tides can be extracted from the rock record. Most of the information contained within this chapter is distilled from two summary papers: Kvale et al. (1999) and Kvale (2006).

To truly understand tidal systems and, in particular, the genesis of tidal rhythmites it is useful to understand both an equilibrium tidal model and a dynamic tidal model. The former explains the driving forces behind the formation of tides and is commonly taught to geology, oceanography, and astronomy undergraduates, whereas the later, more accurately explains real-world tides and is more useful in interpreting the rock record. An understanding of both models is essential to anyone who studies tides and tidal deposits, and both will be discussed.

1.2 Equilibrium Tidal Theory

Most geologists understand tidal periodicities in the context of equilibrium tidal theory. Tides are generated by the gravitational forces of the Moon and, to a lesser degree, the Sun on the Earth. The Moon accounts for approximately 70% of the tide-raising force because of its proximity to the Earth. In an equilibrium world, the Earth is covered by an ocean of uniform depth that responds instantaneously to changes in tractive forces (MacMillan 1966). The equilibrium model can be used to explain five of the six tidal periodicities that have been commonly detected in rhythmite successions. These six cycles are illustrated in Figs. 1.1–1.6 (previously illustrated in Kvale et al. 1998). A seventh cycle known as the "nodal cycle", an approximately 18 year-tidal cycle, and very well documented by Miller and Eriksson (1997) within the Pride Shale, a lower Carboniferous succession found in West Virginia, is not illustrated here.

The figures each illustrate (from upper left to lower right): A diagram and explanation of the equilibrium

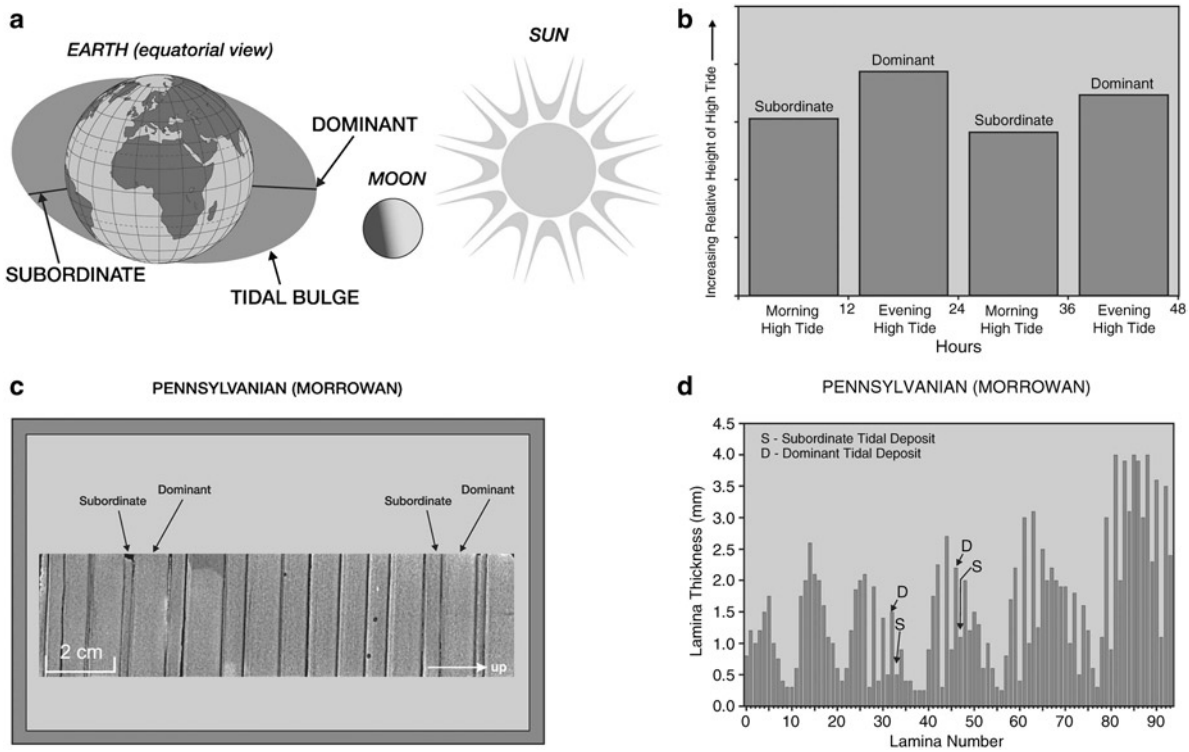

Fig. 1.1 Semidiurnal equilibrium model. (**a**) Two oceanic tidal bulges are produced on opposite sides of the Earth by the gravitational forces of the Sun and the Moon. (**b**) Two tides are produced each day by the spin of the Earth through these bulges. The diurnal inequality is produced when the tidal bulges are not centered above the Earths equator. Semidiurnal tides can be recognized in the rock record by the coupling of thick and thin lamina (**c**) and graphically in the thickness measurements of laminated sequences (**d**) as preserved in the tidal rhythmite succession from the Pennsylvanian Mansfield Formation (Hindostan whetstone beds) from Orange County, Indiana, USA (From Kvale and others (1998) and used by permission from SEPM)

tidal theory of five of the six tidal periods; a bar chart of tidal height data (high tide elevations) from a modern, real-world setting that shows how the astronomical effects are reflected in cyclic changes in daily high tides; a core from an ancient tidal rhythmite succession showing how these cyclic tidal effects might be manifested in a laminated tidal rhythmite; and a bar chart of laminae thicknesses interpreted in the context of the modern tidal cycle.

1.2.1 Semidiurnal (12.42 h)

Within the equilibrium tidal model, the interaction of tidal forces from the Moon and Sun produce two oceanic bulges on opposite sides of the Earth (Fig. 1.1). The rotation of a point on the Earth through these bulges once a day produces two tides (the semidiurnal tide). Typically, these tides are not equal (termed diurnal inequality), as one tide is higher (dominant) than the other (subordinate) because the Moon's orbital plane and the Earth's equatorial plane are not parallel. The angular difference between the two planes is termed lunar declination.

1.2.2 Synodic (29.53 Days)

Daily high tides are higher when the Earth, Moon, and Sun are nearly aligned (full or new moon); this is referred to as "syzygy" (Fig. 1.2). Conversely, lower tides occur when the Sun and Moon are at right angles to the Earth (first or third quarter phase), also known as "quadrature". Tides during full or new moon are referred to as spring tides: "spring" in this context refers to "lively" or "energetic" rather than implying a seasonal connotation. Tides at quarter phases are referred to as neap tides. The neap-spring tidal period

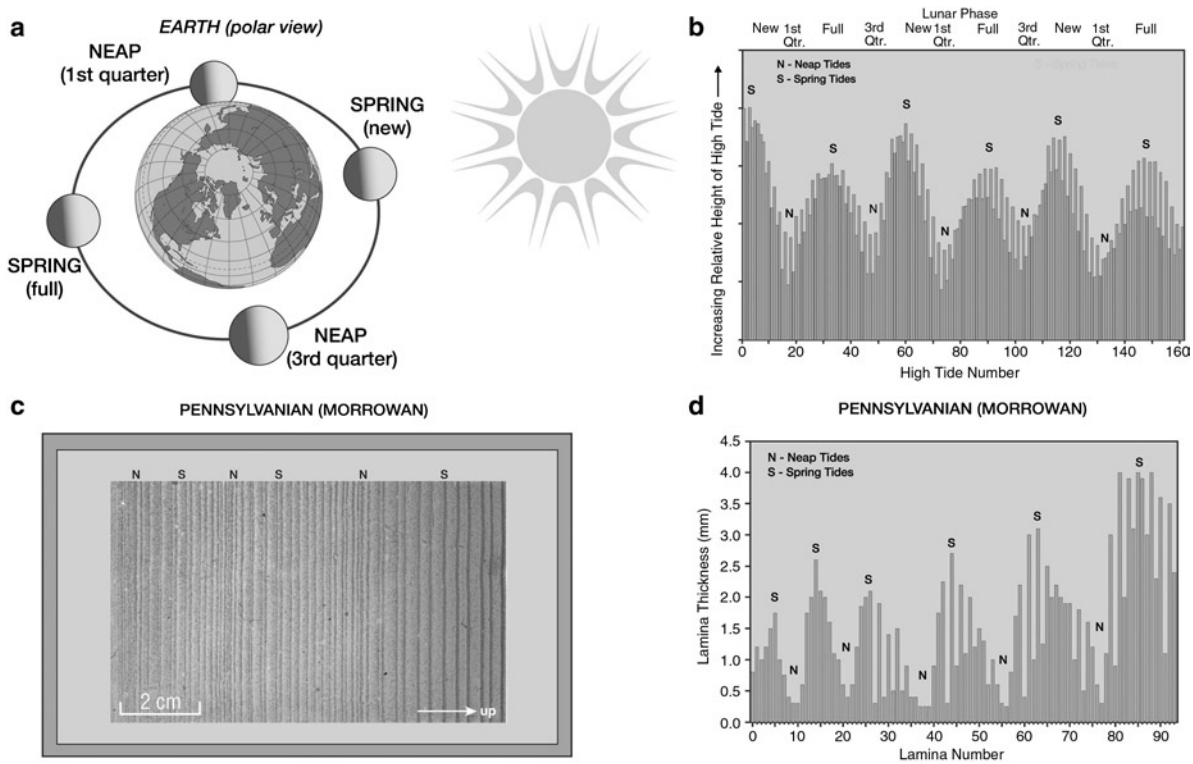

Fig. 1.2 Synodic equilibrium model. (**a**) In an equilibrium tidal model, spring tides occur when the Earth, Moon, and Sun align during full or new moon (also known as "syzygy"). Equlibrium neap tides occur when the Moon-Earth alignment is 90° from an Earth-Sun alignment (also known as "quadrature"). The synodic month (currently 29.53 days) is the time it takes for the Moon to orbit the Earth when measured from a new Moon to the next new Moon. When neap-spring tides can be timed to phases of the Moon they are referred to as "synodic neap-spring tides" (Kvale 2006). (**b**) Graph of tidal heights of a portion of the 1991 predicted high tides for Kwajalein Atoll, Pacific (NOAA 1990) showing the effects of changing lunar phases. (**c**) Portion of a core from the Mansfield Formation (Hindostan whetstone beds), Indiana, USA with neap and spring tidal deposits labeled. (**d**) Measurements of laminae thicknesses from Hindostan whetstone beds with neap and spring tidal deposits labeled (From Kvale et al. (1998) and used by permission from SEPM)

in the equilibrium model is related to the changing phases of the Moon associated with the half-synodic month. The synodic month (new moon to new moon, or full moon to full moon) has a modern period of 29.53 days and encompasses two neap-spring cycles.

1.2.3 Tropical (Semidiurnal, 27.33 Days)

The tidal force also depends on the declination of the Moon (Fig. 1.3). In this usage, "declination" refers to the tilt or angle of the Moon's orbit relative to the Earth's equatorial plane. The period of the variation in declination is called the tropical month – the interval of time it takes the Moon to complete one full orbit from its maximum northern declination to its maximum southern declination and then return. The effect of the tropical month in an equilibrium semidiurnal tidal system is to cause the diurnal inequality of the tides. Ideally, diurnal inequality is greatest when the Moon is at its maximum declination. This inequality is reduced to zero when the Moon is over the equator, producing a crossover in the tidal data (Fig. 1.3). The current length of the tropical month is 27.32 days (2 days shorter than the synodic month – see synodic discussion above). Because of this difference, equatorial passages of the Moon, called crossovers, have a shorter periodicity than the periodicity related to synodic neap-spring tides.

1.2.4 Tropical (Diurnal, 27.32 Days)

In modern, dominantly diurnal systems (primarily one tide per day), the tropical period described above

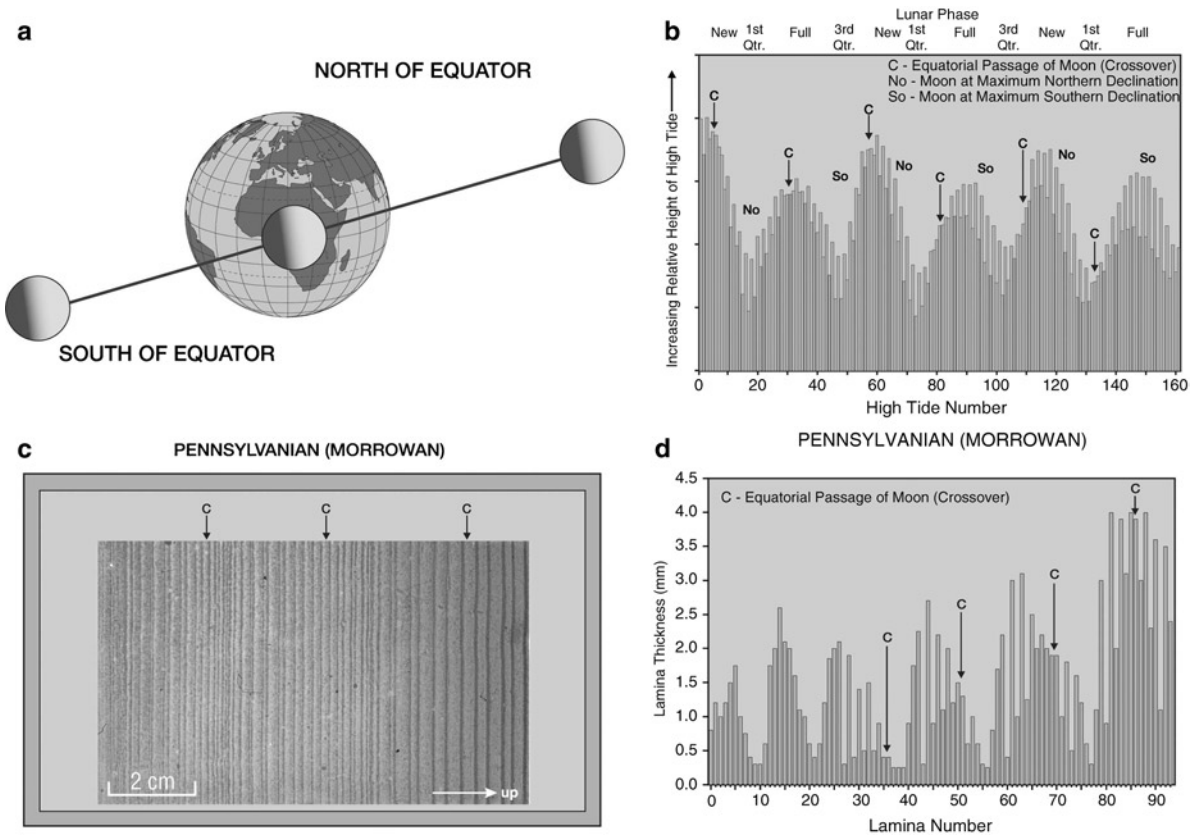

Fig. 1.3 Tropical, semidiurnal equilibrium model. (**a**) Model of the Moon in orbit around the Earth. The lunar declination is exaggerated from its modern range of 18–28°. The tropical month (currently 27.32 days) is the time it takes for the Moon to move from its maximum northern declination to its southernmost declination and back to its northernmost declination in a single orbit. (**b**) Graph of tidal heights of a portion of the same modern tidal record shown in Fig. 1.2b illustrating diurnal inequality of semidiurnal tides. Note diurnal inequality goes to zero when the Moon passes directly over the Earth's equator. (**c**) Image of core shown in Fig. 1.2c showing approximate position (labeled "C") when Moon was above the Earth's equator during deposition. Note the approximate equal thicknesses of the lamina on either side of the *arrow*. (d) *Bar chart* shown in Fig. 1.2d with arrows denoting passages of the Moon above the Earth's equator during deposition (From Kvale et al. (1998) and used by permission from SEPM)

is responsible for generating neap-spring cycles. In contrast to the synodic system, tides in a tropical system behave as though the Sun's gravitational effects are dampened, which is impossible to explain in an equilibrium tidal model (Fig. 1.4). In such cases, the dominant tidal force depends on the declination of the Moon relative to the Earth's equator with the force being greatest when the Moon is most directly over the site in question. In these systems, the predicted and ancient tide data reveal that equatorial passages of the Moon (crossovers) occur in phase with the generation of neap-spring tides, in contrast to the variable relationship exhibited by tropical (semidiurnal) tides.

1.2.5 Anomalistic (27.55 Days)

Another tidal effect arises from the changing distance of the Moon relative to the Earth during the lunar orbit (Fig. 1.5). Because the lunar orbit forms an ellipse, with the Earth slightly offset from the center, the Moon alternates between perigee (closest approach to the Earth) and apogee (the farthest distance from the Earth). During the lunar synodic month there will be two spring tides (see synodic periods described above). These spring tides, however, will be of unequal magnitude producing alternating high-spring and low-spring tides, which correspond to spring tides during or near perigee (high spring) and spring tides during or near apogee (low spring).

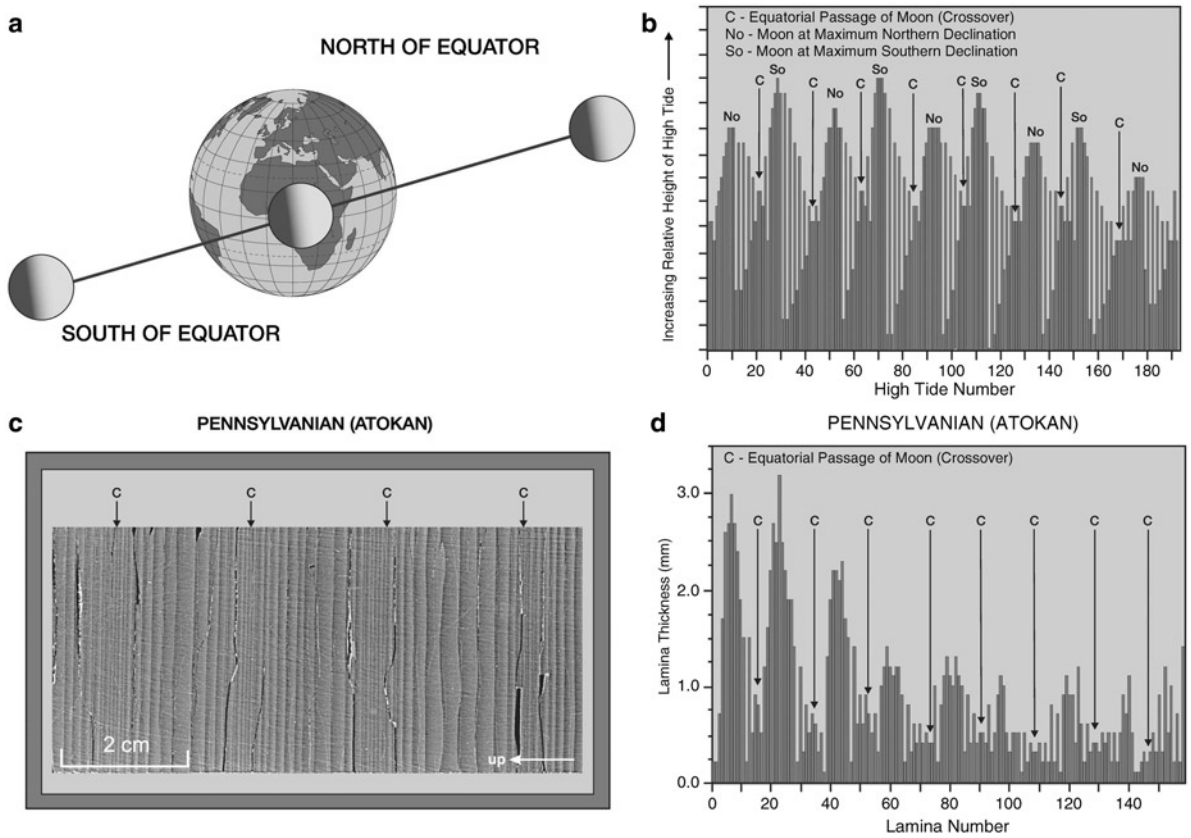

Fig. 1.4 Tropical diurnal model. (**a**) Model of the Moon in its orbit around the Earth (see Fig. 1.3a). (**b**) Graph showing the 1994 predicted relative high tides (mixed, predominantly diurnal) for the Barito River estuary in Borneo (NOAA 1993). Note the passages of the Moon above the Earth's equator perfectly track the neap tides and spring tides to the maximum declinations of the Moon in its orbit around the Earth, a pattern not predicted by equilibrium tidal theory. Such neap-spring tidal cycles are termed "tropical neap-spring tides" (Kvale 2006). (**c**) Photograph of a portion of a core from the Pennsylvanian Brazil Formation, Daviess County, Indiana, USA. *Arrows* indicate lamina deposited with the Moon was above the Earth's equator. (**d**) *Bar chart* of lamina thicknesses measured from core obtained from the Brazil Formation. This unit also is mixed, predominantly diurnal. Note the diurnal inequality of the semidiurnal component goes to zero only in the neap tide deposits. This corresponds to the Moon above the Earth's equator during deposition (From Kvale and others (1998) and used by permission from SEPM)

The semimonthly inequality of the spring tides disappears when the Moon lies along the minor axis of the lunar orbit and the difference in lunar distance is minimized during subsequent spring tides. The time it takes for the Moon to move from perigee to perigee is called the anomalistic month, which is at present 27.55 days.

1.2.6 Semiannual (182.6 Days)

The synodic, tropical, and anomalistic periods have slightly different values. Because of this, these periods will interact constructively twice each year causing tidal forces at these times to reach a maximum (as shown by the dashed line in Fig. 1.6). In the equilibrium tidal model, the date of this tidal maximum is a function of latitude that is related to the declinational effects of the Moon and Sun. An annual inequality has been documented in several ancient tidal rhythmite successions (Kvale et al. 1994). This inequality is interpreted to be climatic (non-tidal) in origin.

1.3 Dynamic Tidal Theory

As noted in the introduction, the equilibrium tidal model explains the driving forces that cause tides but does not explain real-world tides. For instance, the

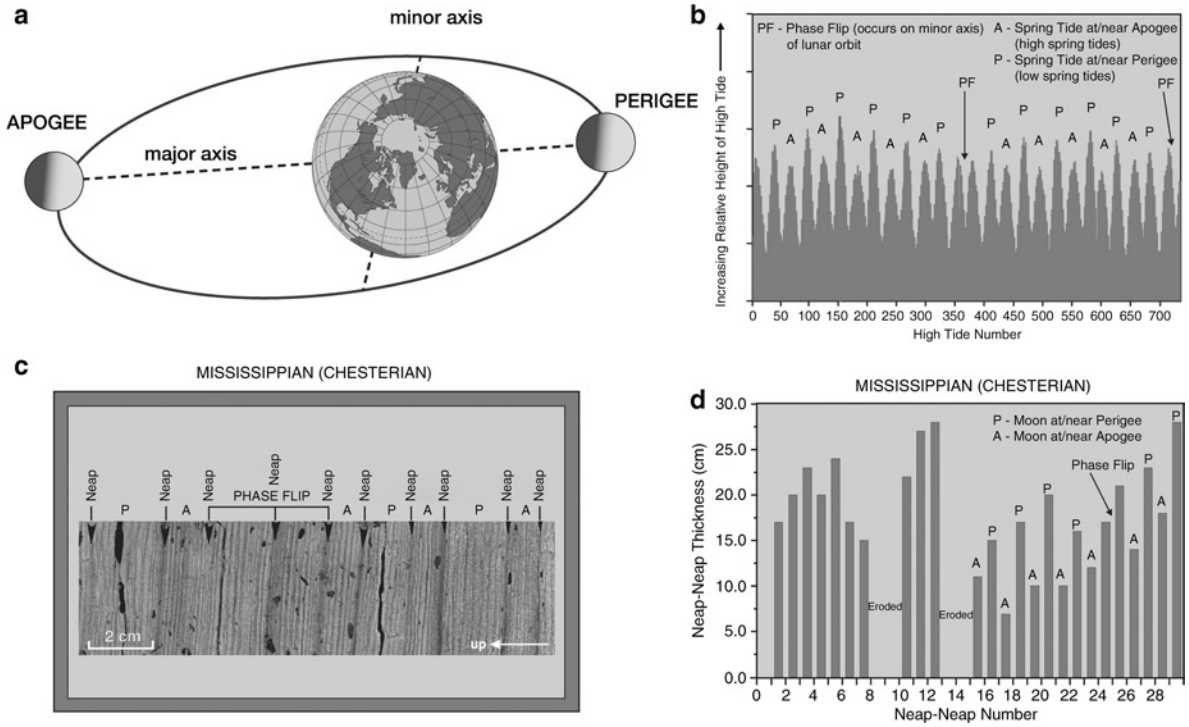

Fig. 1.5 Anomalistic equilibrium model. (**a**) Polar view of the Moon in orbit around the Earth. Note that lunar orbit is not perfectly circular but somewhat elliptical (greatly exaggerated in the diagram) and that the Earth is not position in the direct center of the orbit path. The time it takes for the Moon to go from perigee (closest approach) to apogee (furthest from the Earth) and return is called the "anomalistic month", which is 27.55 days long at present. (**b**) *Graph* showing the 1992 predicted high tides for Saint John, New Brunswick, Canada (NOAA 1991) showing the effects of the anomalistic month on the Saint John tides. Note the semimonthly inequality goes to zero when the Moon and Sun are aligned with the Moon's minor orbital axis (termed "phase flip"). (**c**) Photograph of a core from the Mississippian Tar Springs Formation, Indiana, USA showing the effects of the anomalistic month on neap-spring tidal deposition. (**d**) Graph illustrating thicknesses as measured between neap-to-neap tide deposits from the Tar Springs Formation core, a portion of which is shown in Fig. 1.5c. Note the position of the "phase flip" (From Kvale et al. (1998) and used by permission from SEPM)

world does not spin through two tidal bulges. Instead, oceanic tides rotate as waves around fixed (amphidromic) points within individual ocean basins (Fig. 1.7). Equilibrium tidal theory indicates that diurnal tides should exist only at very high latitudinal positions, which is not the case. For example, the Gulf of Mexico and large tracts in the Indian and western Pacific oceans are dominated by diurnal tides. Tides like those found in Immingham, England, where the semidiurnal tides have minimal diurnal inequality, cannot be explained by equilibrium tidal theory, which requires such tides to exist only in equatorial positions. Finally, equilibrium tidal theory does not explain neap-spring tidal cycles which are synchronous with the 27.32 tropical monthly period such as illustrated in Fig. 1.4.

The difficulties in understanding and explaining real-world tides can be addressed by a dynamic tidal model. This model is built around the concept of a harmonic analysis of the components that compose real-world tides. For instance, the Moon and Sun each generate their own tide within the Earth's oceans. Since the orbits of the Earth around the Sun and the Moon around the Earth are not perfectly circular, the amplitude of the tides generated by each of these bodies, in part, fluctuates depending on the Earth's proximity to the Sun and, much more importantly, the Moon's distance from the Earth. Periodically each of these tides will constructively or destructively interact with each other. The tides associated with changes in Moon-Earth distance or Earth-Sun distance can be considered to be a constituent of the overall tide, which can affect any coastline.

To model these tidal constituents (also known as tidal "species") oceanographers conceptualize each

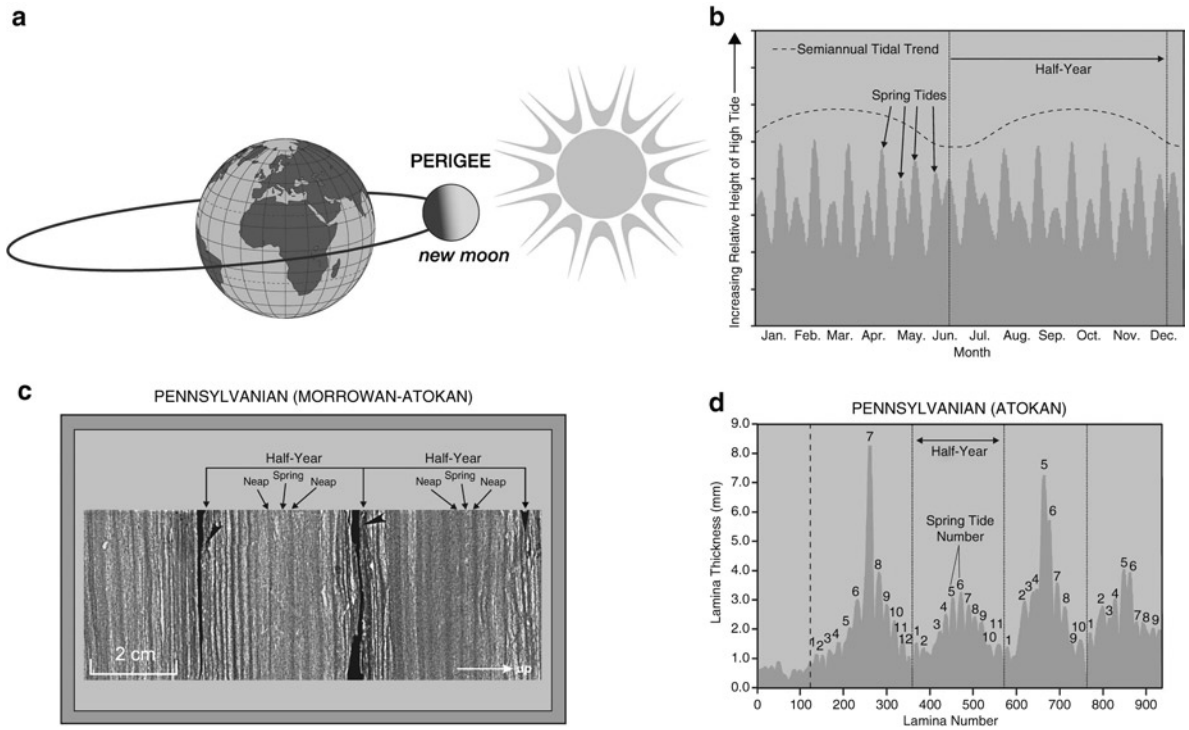

Fig. 1.6 Semiannual equilibrium model. (**a**) View of the configuration of the Earth, Moon, and Sun representing the maximum spring tides formed when the Moon is at perigee, maximum northern declination and new. Such spring tides occur every 182.6 days. (**b**) 1992 predicted high tides from Saint John, New Brunswick, Canada (NOAA 1991) showing the effects of the semiannual convergence of maximum spring tides. (**c**) Photograph of a core from the Pennsylvanian Lead Creek Limestone, Indiana, USA. In this core the neap-spring cycles thicken and thin in a semiannual pattern. (**d**) *Graph* showing the thicknesses of individual lamina from the Brazil Formation, Indiana. These thicknesses are also organized into semiannual tidal cycles. Each number records an individual neap-spring cycle (From Kvale et al. (1998) and used by permission from SEPM)

constituent as a phantom "satellite" that has its own mass (that of the Moon, Sun, or a combination of the two). Each phantom "satellite" has a motion within a plane or is fixed relative to the stars and each generates its own tide with a unique period, response time, and amplitude (Pugh 1987) (Table 1.1). For instance S_2 represents the twice-daily tide generated at a fixed point on the Earth by a "satellite" that has the mass of the Sun in a perfectly circular orbit around the Earth's equator. O_1 represents the daily tide generated at a fixed point on the Earth by a "satellite" with a mass of the Moon and a motion above the Earth's equator. For each of the tidal constituents, the subscript indicates if the tide is diurnal ($_1$) or semidiurnal ($_2$).

The relative intensity for each of these tidal constituents along any oceanic coastline in the world can be determined by a harmonic decoupling of an extended hourly tidal record. These measurements typically are recorded in most major harbors and other tidal stations around the world. More than 100 tidal constituents have been identified from a harmonic extraction of Earth's tides, however, seven of these (Table 1.1) account for more than 80% of any real-world tide (Defant 1961). The resonate amplification or destruction of these tidal constituents determines the resulting tide for a specific area within the Earth's oceans (Fig. 1.8).

As noted above, each of these tidal constituents corresponds to a unique tidal wave. These waves do not travel around the world as predicted by equilibrium tidal theory, but rather rotate around a point (referred to as an "amphidromic point") within a region of the ocean at a speed determined by their constituent's orbital periodicity or the periodicity of the Earth's spin (Fig. 1.7). The location of these points is determined by basin geometries and the Coriolis force.

Ideally, amphidromic circulation should be counterclockwise in the Northern Hemisphere and clockwise in the Southern Hemisphere and never on the equator

but, as shown above, real-world tides don't always follow convention and exceptions are known (Open University Course Team 1999).

The major tidal cycles discussed under the equilibrium model can be understood in the context of the dynamic model and tidal constituents. Specifically, the synodic neap-spring cycle is generated through the interaction of the S_2 and M_2 constituents. In the modern world, these two tides come into phase and amplify the resulting tide every 14.77 days. The result is a synodic spring tide. Conversely, every 13.66 days K_1 and O_1 converge and generate a tropical spring tide. Whether a spring tide along a specific coastline is dominated by the synodic spring tide or the tropical spring tide is determined by the basin geometry. For instance, the Gulf of Mexico is dominated by the K_1 and O_1 tides, therefore neap-spring tides cycle with the tropical month (Fig. 1.9). The east coast of the USA, however, is dominated by S_2 and M_2 tides resulting in neap-spring tides that cycle with the synodic month (Fig. 1.9). The semimonthly inequality of spring tides occurs because of the convergence of M_2 and N_2 every 27.55 days. A diurnal inequality is driven by the interaction of O_1 and M_2 (in phase once a day) and is noted in coastal tides when these constituents are of sufficient amplitude.

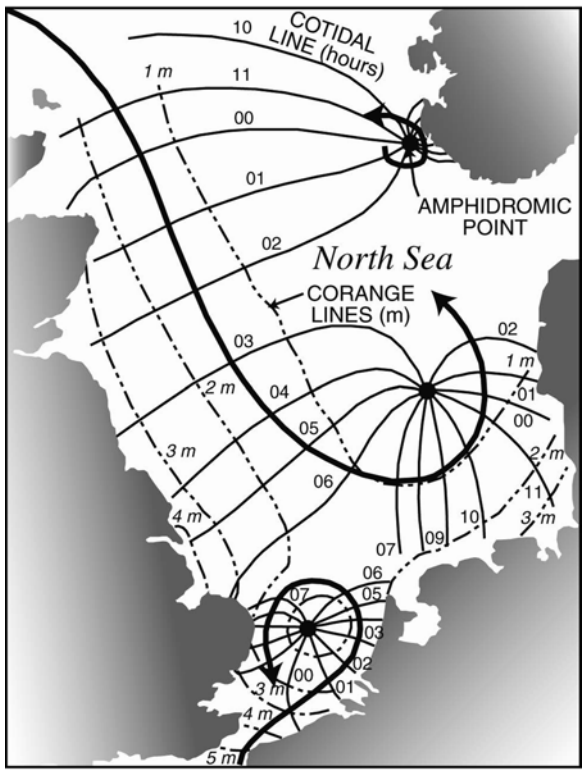

Fig. 1.7 Diagram showing the amphidromic circulation for the M_2 tide in the North Sea. Co-tidal lines indicate times of high water. And co-range lines indicate lines of equal tidal range. Figure is modified from Dalrymple (1992) which was based on a map first drawn by J. Proudman and A. T. Doodson (From information found in Cartwright 1999) (From Kvale (2006) and used by permission from Marine Geology)

One can look at the progressive change in relative intensity of particular tidal constituent along a coast and see how that affects the resulting tides. For example, Figs. 1.10 and 1.11 shows the amplitudes for the seven dominant tidal constituents for the Gulf of Carpentaria, Australia and the tidal patterns that result from changes in the relative amplitudes of the various constituents (from Kvale 2006). At the mouth of the gulf at Booby Island, the tides are dominated by M_2, K_1 and O_1. Given the dominance of O_1 and K_1, the neap-spring cycle occurs every 27.32 days and corresponds to the tropical monthly period. However, unlike many regions whose neap-spring cycles are tropically driven, there is a relatively strong M_2 tide (but relatively weak S_2 tide) at the mouth of the gulf. The resultant

Table 1.1 List of the seven most common tidal constituents, their rotational speed (number of degrees a tidal wave generated by the constituent can travel around its amphidromic point in 1 h), description, and period in solar hours (Defant 1961)

Tidal constituent	Speed (degrees/hour)	Origin	Period in solar hours
M_2	28.9841	Principal lunar	12.42
S_2	30	Principal solar	12
N_2	28.4397	Larger elliptical lunar	12.66
K_2	30.0821	Combined declinational lunar and declinational solar	11.97
K_1	15.0411	Combined declinational lunar and declinational solar	23.93
O_1	13.943	Principal lunar	25.82
P_1	14.9589	Principal solar	24.07

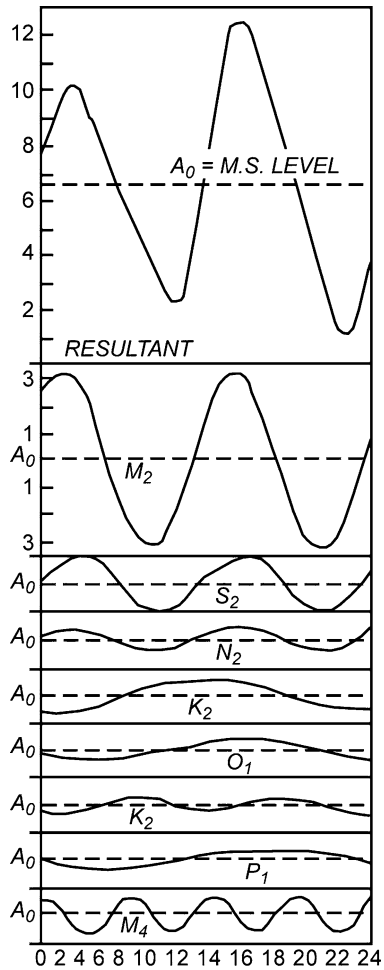

Fig. 1.8 Resulting tide predicted from the stacking of 9 different tidal constituents. Horizontal units are in hours (Modified from MacMillan, 1966 in Kvale, (2006) and used by permission from Marine Geology)

tide at Booby Island exhibits a tropically driven neap-spring cyclicity comparable to the tide depicted in Fig. 1.4 except that it also exhibits a strong semidiurnal component that is driven by M_2. Progressing further south into the Gulf of Carpentaria, the strengths of K_1 and O_1 increase relative to M_2 creating a tide that is dominantly diurnal.

1.4 Ancient Tides

Some tidal rhythmites in the rock record preserve long (several months worth), relatively complete successions of daily or semidaily tidal deposition. Particularly complete records can be interpreted in the context of the dynamic tidal model and several examples are noted below.

1.4.1 Hindostan Whetstone Beds (Pennsylvanian, Indiana)

Figures 1.2 and 1.3 show both a segment of core and a bar chart of the laminae thicknesses from the Hindostan Whetstone beds found in Orange County, Indiana (Kvale et al. 1989). Neap-spring cycles in this chart occur more frequently than crossovers indicating that these tides were synodically driven and hence related to the dominance of the M_2 and S_2 over the O_1 and K_1 constituents. Some caution is needed, however, in interpreting crossover patterns because the absence of a single half-day event could cause an apparent crossover. Ways to infer completeness of a tidal pattern are discussed by Kvale et al. (1999). Suffice it to state that with suitably long tidal rhythmite records, such as presented here, it is possible to interpret crossover patterns with some confidence.

This example clearly shows a diurnal inequality, and, as such, O_1 must be significant. There appears to be a lack of a pronounced semimonthly inequality (anomalistic cycle) suggesting that N_2 was relatively weak. Therefore, tides that deposited the Hindostan Whetstone beds were dominated by the constituents M_2, S_2, and O_1 followed by K_1 and N_2.

1.4.2 Brazil Formation (Pennsylvanian, Indiana)

Figure 1.4 show a segment of core and a bar chart of laminae thicknesses from the Brazil Formation of Daviess County, Indiana (Kvale and Archer 1990; Kvale and Mastalerz 1998). The neap-spring cycles in this example occur at the same frequency as the crossovers indicating that these tides were driven by the tropical period and hence reflect a dominance of O_1 and K_1 over S_2 and M_2. A weak semidiurnal signal occurs during the neap tides and indicates that M_2 had some amplitude and importance in the resulting tide. The Brazil Formation rhythmites, like the whetstone beds discussed above, lack a prominent semimonthly inequality suggesting a weak N_2 tidal constituent. It can be inferred from this data base that the Brazil

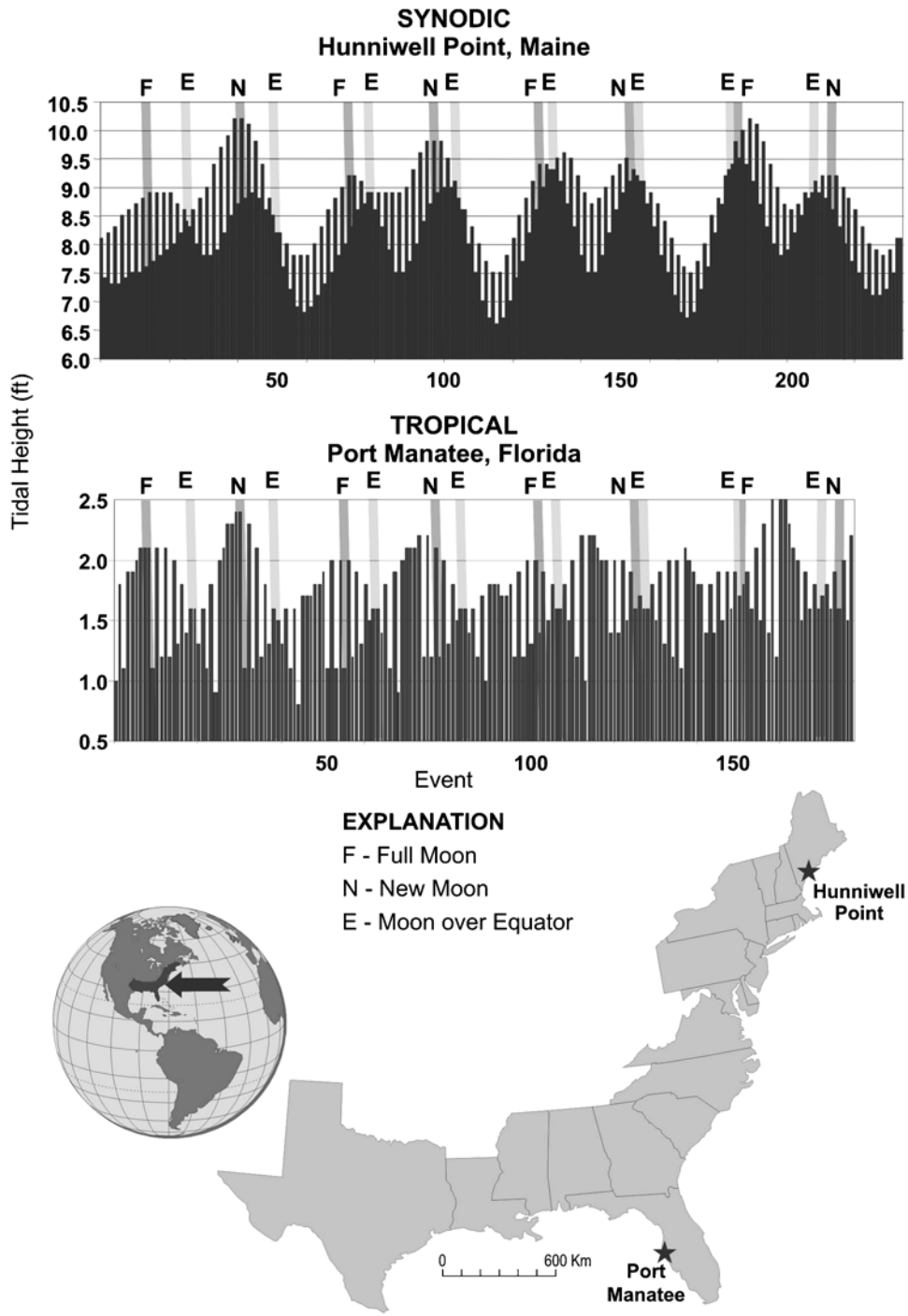

Fig. 1.9 Graphs showing predicted high-data for two tidal references stations from the east coast and Gulf coast USA. The Port Manatee example is typical of the tides in the Gulf coast and the Hunniwell graph typifies east coast tides. Both tidal records cover the same interval of time from January through early May, 2005 (National Oceanographic and Atmospheric Administration Web site 2004). Note that the equatorial passages of the Moon are fixed with the neap tides in the Gulf coast station but move through the graph in the east coast example. As such, Gulf coast neap-spring tides are driven by the tropical month but the east coast neap-spring tides are controlled by the phase changes of the Moon associated with the synodic month (From Kvale (2006) and used by permission from Marine Geology)

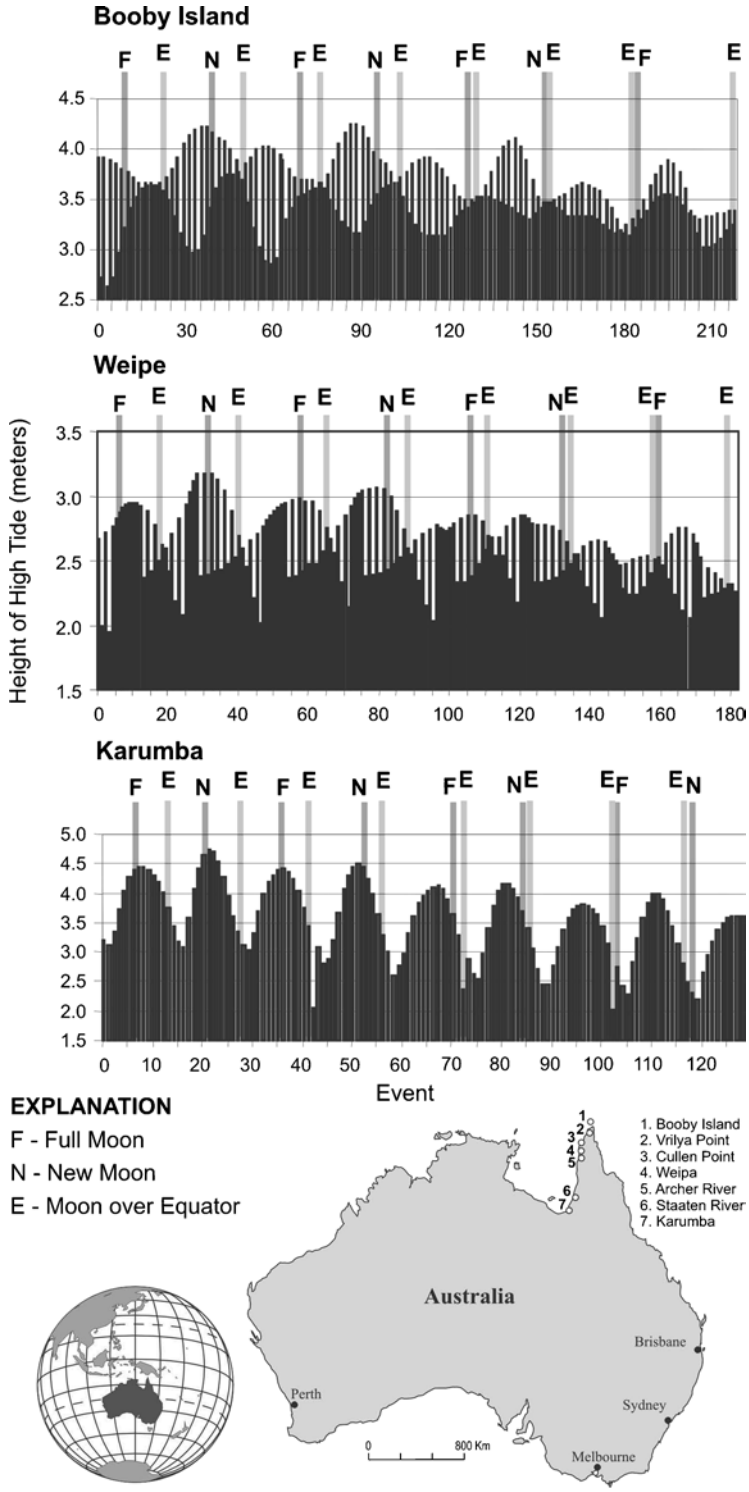

Fig. 1.10 Graphs and location map for predicted high-tide data from three tidal reference station in the Gulf of Carpentaria, Australia. The time interval for each graph spans January through early June, 2004 (Australian National Tidal Centre, Bureau of Meteorology Web site, 2004) (From Kvale (2006) and used by permission from Marine Geology)

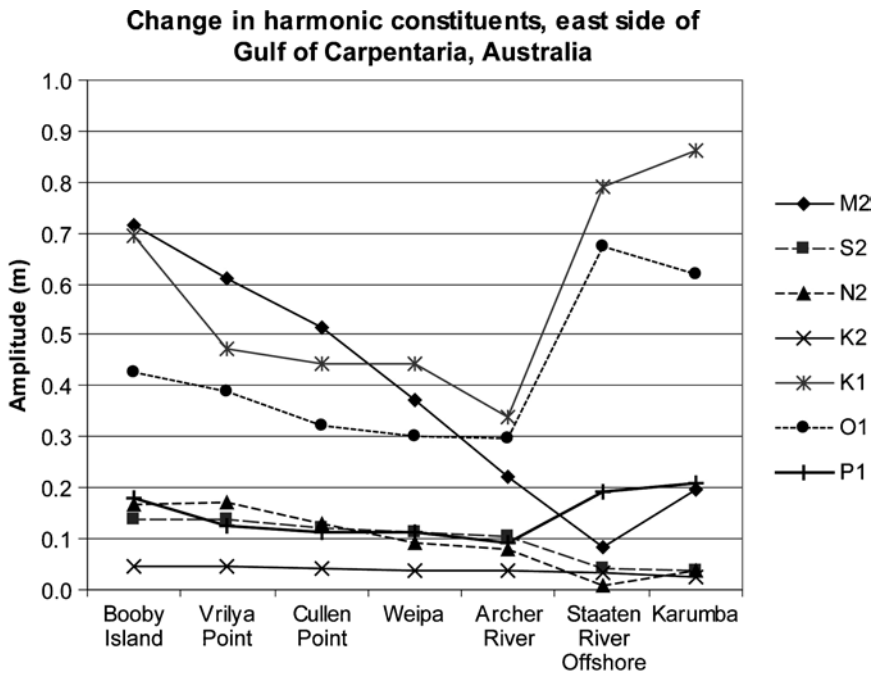

Fig. 1.11 Line graph showing the changes in tidal amplitude for the seven most dominant tidal constituents for several tidal reference stations located along the eastern side of the Gulf of Carpentaria (locations noted in Fig. 1.10. Constituent data was extracted using the Seafarer Tides software package by the Australian National Tidal Centre, Bureau of Meteorology and provided to Kvale (2006) (From Kvale (2006) and used by permission from Marine Geology)

Formation tides were dominated by O_1, K_1, followed by M_2 with very weak contributions from S_2 and N_2.

1.4.3 Abbott Sandstone (Tradewater Formation, Pennsylvanian, Illinois)

Figure 1.12 shows an outcrop and bundle thicknesses from some flaggy, large-scale tidal bundles along Interstate 57 in Johnson County, Illinois (Kvale and Archer 1991). A histogram of bundle thicknesses indicates a strong semidiurnal signal throughout the record. While not as clean a tidal record as the two previous examples, the Abbott sandstone example appears to exhibit minimal diurnal inequality during the neap tides. When the diurnal inequality tracks neap tides, it indicates that neap-spring cyclicity is driven by the tropical period (e.g. Fig. 1.4). As such, the Abbott Sandstone tidal record resembles that of Booby Island, Australia (Fig. 1.10), in which M_2, O_1 and K_1 dominate the resultant tide over S_2. There is a suggestion of a semimonthly inequality to the Abbott sandstone record indicating that N_2 was stronger than S_2 and sufficiently strong to influence the tidal record.

These examples illustrate that tidal constituents can be extracted from the rock record in well-preserved tidal rhythmites. While it is not always possible to draw conclusions regarding so many tidal constituents, deposits can generally be determined to be either diurnal or semidiurnal in nature based on the absence or occurrence of alternating thick-thin laminae. Most, but not all, semidiurnal tidal deposits can be related to the synodic period and the convergence of M_2 and S_2 constituents. Exceptions of semidiurnal, tropically driven neap-spring tides or tidal deposits, such as Booby Island and the Abbott Sandstone, are known and can be discerned if the tidal record is long and clean enough. All diurnal deposits should have been deposited in tropically driven neap-spring cycles. Semidiurnal depositional systems that lack strong K_1 or O_1 constituents (like Effingham, England), and in which tidal sediments were deposited only on high intertidal zones might mimic a diurnal tidal deposit (Archer and Johnson 1997). In such a case, additional outcrop work might result in the discovery of lower intertidal or subtidal facies that would resolve the issue.